JACS
JOURNAL OF THE AMERICAN CHEMICAL SOCIETY

Communication

pubs.acs.org/JACS

Fractal Etching of Graphene

Dechao Geng,† Bin Wu,† Yunlong Guo, Birong Luo, Yunzhou Xue, Jianyi Chen, Gui Yu,* and Yunqi Liu*

Beijing National Laboratory for Molecular Sciences, Institute of Chemistry, Chinese Academy of Sciences, Beijing 100190, P. R. China

Supporting Information

ABSTRACT: An anisotropic etching mode is commonly known for perfect crystalline materials, generally leading to simple Euclidean geometric patterns. This principle has also proved to apply to the etching of the thinnest crystalline material, graphene, resulting in hexagonal holes with zigzag edge structures. Here we demonstrate for the first time that the graphene etching mode can deviate significantly from simple anisotropic etching. Using an as-grown graphene film on a liquid copper surface as a model system, we show that the etched graphene pattern can be modulated from a simple hexagonal pattern to complex fractal geometric patterns with sixfold symmetry by varying the Ar/H_2 flow rate ratio. The etched fractal patterns are formed by the repeated construction of a basic identical motif, and the physical origin of the pattern formation is consistent with a diffusion-controlled process. The fractal etching mode of graphene presents an intriguing case for the fundamental study of material etching.

Material etching refers to the spontaneous removal of building blocks from a material matrix by physical or chemical approaches, and in many cases it can be considered as the reverse of the growth process from the microscopic point of view. Understanding the etching process is essential for the design of materials and the realization of their useful functionality. Both material growth and etching require a high-energy-barrier nucleation process and then an easier pathway for enlarging the formed nuclei. In general, controlling the process parameters can result in the spontaneous formation of thermodynamically stable ordered structures and can also afford various kinetically controlled metastable structures with high-energy crystalline facets or edges. This control has been verified for many material growth systems with a length scale from the nanometer to micrometer to macroscopic scale.[1−3] The family of snowflakes is a fascinating example with rich patterns formed by a nonlinear process provided by nature.[4] In contrast, it is commonly accepted that perfect crystalline materials (e.g., single-crystal Si) are etched through a simple anisotropic rule,[5] leading to simple thermodynamically stable etched patterns with Euclidean geometries. The underlying physical mechanism originates from the different etching rates along different crystallographic surfaces or directions associated with different free energies. However, etched structures of materials beyond simple Euclidean geometries have not been proposed and demonstrated.

Graphene, which can be viewed as a perfect two-dimensional (2D) single-layer atomic crystal, has attracted much attention because of its superstability under ambient conditions and its excellent physical properties.[6,7] The single layer of C atoms with good crystallinity provides the simplest model system to study fundamental growth and etching processes. Intensive efforts have been devoted to the development of strategies to grow high-quality graphene with controlled size, crystallinity, and edge structures[8−11] by the chemical vapor deposition (CVD) method. On the other hand, many studies of graphene etching have concluded that it essentially follows a similar anisotropic rule regardless of the use of different etchants such as hydrogen plasma,[12−15] H_2[16,17] or metal nanoparticles.[18−21] This etching mode leads to preferential etching along the zigzag direction[13] in the graphene lattice, producing either hexagonal holes or line patterns with an angle of 60° between them.[18,20] We recently discovered a full spectrum of graphene crystal patterns that can be finely controlled simply by tuning the composition of an inert gas and H_2 during the growth.[22] In view of the similarity between the growth and etching processes, these findings inspired us to re-examine the fundamental issue of the graphene etching mode.

Here we report the first observation of a collection of previously unrevealed etched graphene patterns with sixfold symmetry, ranging from a simple Euclidean hexagon to complex fractal shapes. Our experimental results strongly indicate that the universal diffusion-controlled mode that is well-known in the crystal growth of various material systems[1−4,22] is also responsible for the formation of etched graphene patterns, providing a generally effective approach for engineering of the final etched patterns of other 2D or 3D materials. To test the intrinsic graphene etching behavior, we started by preparing graphene monolayer films or separated individual graphene flakes on a liquid copper surface using a recently developed method.[11] Briefly, a Cu/W substrate was heated to a temperature higher than the melting point of Cu (1080 °C; we explored temperatures in the range 1100−1160 °C) and then annealed for 20 min in pure H_2. A monolayer graphene film was then grown on the surface of the liquid copper using CH_4 in Ar/H_2 as the carrier gas at ambient pressure for ∼30 min. In the normal experiments on graphene film growth, the CH_4 source was then switched off, and the system was cooled to room temperature. In the etching experiments, after the CH_4 source was turned off, the Ar/H_2 flow was continued for a period of time at a particular flow rate ratio while keeping the temperature the same. Various Ar/H_2 flow rate ratios were explored to study the effect of the flow rate ratio on the etched graphene pattern. Finally, the furnace was opened, allowing the system to cool rapidly to room temperature

Received: March 2, 2013

   dx.doi.org/10.1021/ja402224h | J. Am. Chem. Soc. XXXX, XXX, XXX−XXX

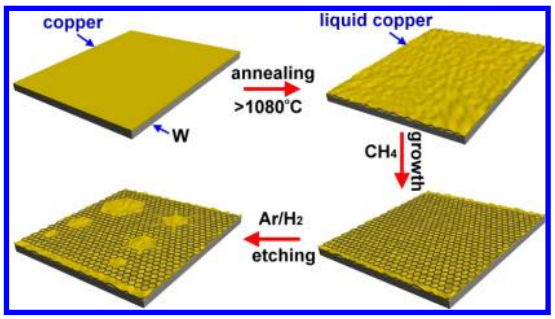

Figure 1. Schematic showing the process of graphene growth on a liquid copper surface by CH_4 CVD and subsequent etching using H_2 in Ar.

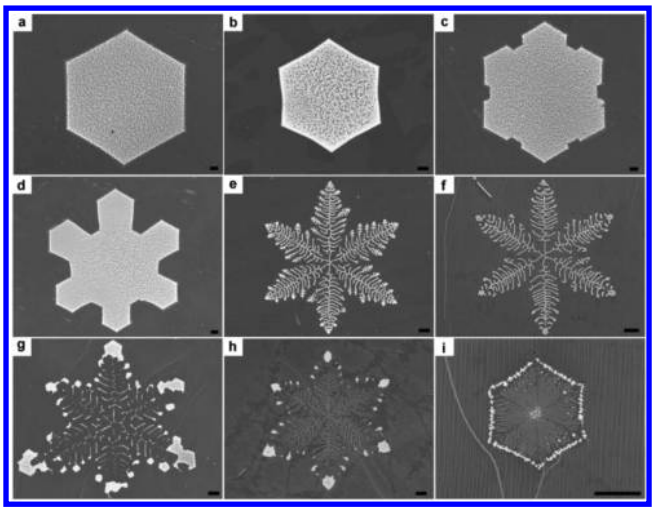

Figure 2. Typical SEM images of a series of etched graphene patterns with different shapes obtained using various Ar/H_2 flow rate ratios. The different conditions are summarized in Table S1. It should be noted that all of the structures show hexagonal symmetry. All scale bars are 5 μm.

(~100 °C/min). The whole process is illustrated schematically in Figure 1.

Figure 2 shows a series of scanning electron microscopy (SEM) images of typical individual etched patterns obtained at various Ar/H_2 flow rate ratios [see Table S1 in the Supporting Information (SI)]. In all these cases, the monolayer graphene film was grown on a liquid Cu surface using CH_4 at 0.3 standard cubic centimeters per minute (sccm), 20 sccm H_2, and 800 sccm Ar for 30 min at 1160 °C at ambient pressure. These conditions ensured the formation of a monolayer graphene film. When a low Ar/H_2 flow rate ratio (800 sccm/100 sccm) was used in the etching stage, hexagonal holes (white area in Figure 2a) were observed on the as-grown graphene film (dark area in Figure 2; also see the characterization below). This observation is consistent with those reported previously.[12−17] As the Ar/H_2 flow rate ratio gradually increased, the edge of hexagonal etched area started to curve toward the center (Figure 2b). The trend is remarkably analogous to the evolution of the graphene crystal shape when the similar modulating method is used.[22] Further increasing Ar/H_2 ratio led to hexagon-shaped etched structure with six protruding arms (Figure 2c), and these arms gradually became more prominent with the whole structure more opened (Figure 2d). It should be noted that the detailed structures in Figure 2c,d are quite different from those observed in graphene crystal growth patterns.[22] At a flow rate ratio of 800 sccm/20 sccm, a very finely carved fractal structure similar to a snowflake morphology was produced (Figure 2e). The main features of this

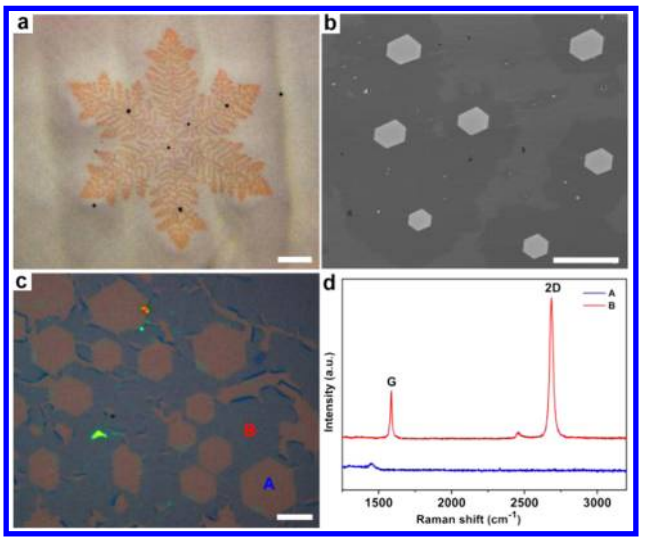

Figure 3. Characterizations of etched graphene structures. (a) Typical optical image of an etched fractal pattern on a Cu surface. The optical contrast between the snowflake-like etched region and the graphene region is due to oxidation of the Cu surface in air. (b, c) Typical SEM images of separated etched hexagonal holes in a graphene film (b) before and (c) after the film was transferred onto a 300 nm SiO_2/Si substrate. Labels A and B in (c) indicate etched and graphene film regions, respectively. (d) Raman spectra of regions A and B in (c). All scale bars are 10 μm.

kind of etched structure essentially remained the same until a strikingly different structure appeared at a very high flow rate ratio of 800 sccm/3 sccm (Figure 2i). In this case, all of the etched lines in each of the six triangles of the hexagon are aligned along one direction. It is worth mentioning that in each case the individual etched structures were formed in a high yield and uniformly dispersed on the surface (Figure S1 in the SI), demonstrating the high reproducibility of the etching behavior.

The above etched patterns were confirmed by further characterizations. An optical image of a snowflake-like etched structure (Figure 3a) shows the commonly observed contrast between monolayer graphene (brighter region) and the Cu surface (darker region) due to the oxidation of Cu surface in air.[23] Graphene films with etched patterns were also transferred onto 300 nm SiO_2/Si substrates. Figure 3b,c shows SEM images of a film before and after transfer using an electrochemical method[24] (see Methods in the SI), respectively. Figure 3d displays Raman spectra of the areas labeled B and A in Figure 3c. The spectrum of B is characteristic of single-layer graphene [a symmetric 2D peak located at 2698 cm^{-1} with a full width at half-maximum of 35−40 cm^{-1} and a large intensity ratio of the 2D and G bands (I_{2D}/I_G = 2.5−4)], whereas the spectrum of A contains no graphene signal. The small peak located at 1452 cm^{-1} in the spectrum of A comes from the SiO_2 substrate, as confirmed by the presence of the same peak in the Raman spectrum of the bare substrate. These measurements provide direct evidence of the graphene etching during the process and are also consistent with the experimental fact that a longer etching time (10−20 min) eventually led to the complete removal of the graphene film in all cases.

From Figure 2 and the above analysis, it is intriguing that different etched patterns clearly exhibit the evolution from simplicity to complexity or Euclidean to fractal geometry in a real system. The pattern family is an exception to the simple anisotropic etching behavior previously observed for other crystalline materials[5] and graphene.[12−21] To test the generality of

dx.doi.org/10.1021/ja402224h | J. Am. Chem. Soc. XXXX, XXX, XXX−XXX

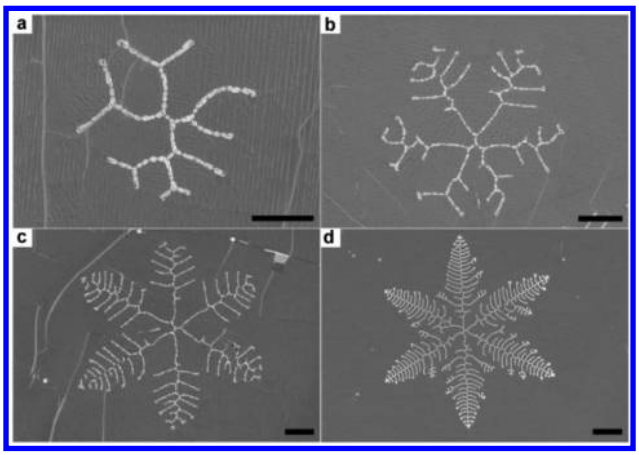

Figure 4. Evolution of etched graphene patterns recorded on the same sample under the conditions for Figure 2e shown in Table S1. All scale bars are 5 μm.

this graphene etching mode and its physical origin, we further explored the roles of temperature, etching time, and catalyst type in the process. Changing the temperature over the range from 1100 to 1160 °C essentially resulted in the same etching behavior (Figure S2). When brass (copper alloy, 30% Zn and 70% Cu) was used as the liquid catalyst, we also found a similar evolution of etching patterns at an etching temperature of 1100 °C. These investigations provided strong evidence for the generality of this etching mode.

From the geometric point of view, the etched patterns can be described by fractal geometry. Indeed, fractals are universal in natural and societal phenomena and occur on all length scales from galactic to nanometer.[25] Developed complex structures can be considered to form simply by repeated construction of a basic identical motif. As the initial etching points did not start simultaneously in the case of graphene etching, the set of separate etched patterns on the same sample actually represented a collection developed at different stages. Different structures in Figure 4 recorded on the same sample thus showed how the simple structure developed into the complex fractal as a function of time. The etched pattern at the early stage contained simple branched lines (Figure 4a), and then a similar line structure was repeatedly constructed into the existing structure, gradually forming a fractal one (Figure 4b–d). The anisotropic etching rule for the basic motif (Figure 4a) was not strictly followed, as reflected by the deviations from straight lines and the angles of 120° or 60° between etched lines. However, the symmetry and self-similarity of the patterns indicate that the etching did occur along the preferential crystalline direction, but with a detectable uncertainty. The fractal dimensions of the patterns in Figure 4 apparently fall between 1 and 2.

Despite the complexity of the etched pattern family, the general physical origin of the pattern formation and evolution can be understood in a qualitative way. The shape features, including branching, self-similarity between the part and the whole, negative edge curvature, and protruding parts, are characteristic of a diffusion-controlled process.[1−4,22] Suppose that graphene etching events start at random points by removal of C atoms from graphene lattice, thus developing a small hole in graphene film. Subsequent etching pathways mainly depend on two competing rates:[26] the rate of etching along the perimeter of the etched holes to find the most energetically favorable sites and the rate of etchant diffusion to the etched area. In general, fast diffusion of the etchant impedes the most energetically favorable removal of C atoms, leading to a branched structure. The degree of branching or curvature is directly related to the relative ratio of the two rates.

Under the guidance of this general picture, we can analyze the real etching system in a simplified manner and provide possible explanations for detailed observations in the graphene etching experiments. Suppose that H_2 or dissociated H radicals are active etchants for graphene. A high Ar/H_2 flow rate ratio leads to less coverage of the active etchants on a supported surface, possibly favoring fast surface diffusion and fractal etched patterns. There are two possible surfaces for etchant diffusion: graphene and liquid Cu. Because of higher surface free energy of liquid Cu, etchants are expected to be more readily adsorbed and diffused on the liquid Cu surface than on the graphene surface. In fact, different experimental results for etching on boundaries of the graphene film and within the graphene film revealed that it was necessary for the active etchants to diffuse on the liquid Cu surface to start effective etching. For example, we found that etching preferentially occurred at the rugged edge locations of graphene film and then extended a line structure into the graphene region (Figure S3). However, as shown in Figures 2 and 4, etched patterns started from a point within the graphene film and then developed into the entire symmetric structure. Moreover, the length of the etched lines starting from the edge of the graphene (>100 μm with an estimated etching rate of 20−30 μm/min; Figure S3) was usually longer than that within the film (several tens of micrometers with an estimated etching rate of 5−12 μm/min in a diagonal direction), indicating the etching rate difference in these two cases. If the etchants around the area of the initial etched holes are supplied by diffusion on the graphene surface or directly from free space in the reaction chamber, no difference would be expected in the two cases (also see the schematic diagram of etchant diffusion on surfaces in Figure S4). In the case of etching occurring within the graphene film, the low etching rate is likely due to low etchant concentration and hindered surface diffusion within the confined space between the Cu surface and the graphene film. Etchant diffusion on an isotropic liquid Cu surface further provides the physical origin of the high symmetry of the etched fractal patterns. It is also important to point out that the etched line structure due to diffusion-controlled etching is different from that of nanoparticle etching.[18−21] In that case, the line width is related to the nanoparticle size, and the nanoparticle's motion results in the etched profile. In addition, the small hexagonal holes observed at the edges of the patterns shown in Figure 2g–i appeared to be different from their corresponding main structures. It should be noted that these hexagonal holes were formed during the end of etching process. The formation of these hexagonal holes may have involved complicated non-steady-state conditions as the system was rapidly cooling down.

The etching of individual graphene domains revealed several interesting points. First, the etched hexagonal holes are within single graphene flakes (Figure S5). Different etched patterns are clearly oriented, and the edges are parallel to the edges of the graphene flake. Transmission electron microscopy (TEM) measurements (Figure S6) were also performed on a transferred graphene film, and large single-crystalline regions in the film were found, consistent with the previous observation that the continuous film was formed by the connection of individual single domain graphene flakes.[11] These results can explain frequent observations of aligned etched patterns within graphene films (Figures 3b and S1). This technique could be very useful for

dx.doi.org/10.1021/ja402224h | J. Am. Chem. Soc. XXXX, XXX, XXX−XXX

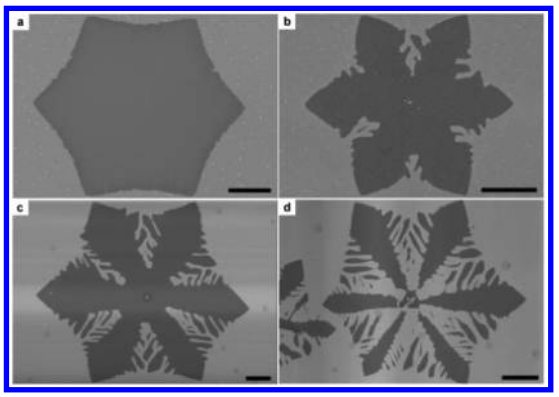

Figure 5. Evolution of etched patterns on individual graphene flakes recorded as a function of etching time: (a) 0 min; (b) 3 min; (c) 5 min; (d) 8 min. Etching conditions: Ar/H_2 (800 sccm/20 sccm) at 1100 °C. All scale bars are 10 μm.

identifying the graphene crystallinity and edge structure since it has been proven that the edge of an etched hexagon has a zigzag structure.[13] Second, Figure 5 shows the etching behavior of individual graphene flakes grown on a liquid brass surface as a function of etching time. Etching from the edge is clearly the dominant pathway for individual flakes, consistent with the above analysis that the process of surface diffusion of the etchants determines the etching pathway and etching rate. As the etching time increased, the individual graphene flake was gradually etched away, forming snowflake-like graphene patterns similar to the graphene crystal patterns supposed to be formed during the growth reported in our previous work.[22] Although the temperatures used to grow snowflake-like graphene crystal patterns (1050−1080 °C)[22] were lower than those in this study, the etching may indeed play an important role in shaping the graphene morphology in this very complicated growth and etching system. This speculation is expected to be experimentally tested when the technique for in situ observation of graphene growth is developed in the future.

In summary, previous studies have shown that graphene etching using various etchants, including hydrogen plasma, H_2, or metal nanoparticles, follows an anisotropic rule, leading to either hexagonal holes or line patterns with 60° angles between them. The resulting etched patterns have characteristics of simple Euclidean geometry. Here we have demonstrated for the first time that etched graphene patterns can be complex and fractal instead of commonly accepted simple and Euclidean. The experimental results provide evidence of a diffusion-controlled etching mode. This discovery represents an unrevealed intrinsic graphene etching mode that may apply to a wide range of other 2D or 3D material systems.

■ ASSOCIATED CONTENT

Ⓢ Supporting Information

Methods and additional figures. This material is available free of charge via the Internet at http://pubs.acs.org.

■ AUTHOR INFORMATION

Corresponding Author

liuyq@iccas.ac.cn; yugui@iccas.ac.cn

Author Contributions

[†]D.G. and B.W. contributed equally.

Notes

The authors declare no competing financial interest.

■ ACKNOWLEDGMENTS

This work was supported by the National Basic Research Program of China (2011CB932700, 2011CB808403, 2011CB932303, and 2009CB623603), the National Natural Science Foundation of China (61171054, 21273243, 60911130231, 51233006, and 61101051), and the Chinese Academy of Sciences.

■ REFERENCES

(1) Satio, Y. *Statistical Physics of Crystal Growth*; World Scientific: Singapore, 1996.
(2) Roder, H.; Hahn, E.; Brune, H.; Bucher, J.; Kern, K. *Nature* **1993**, *366*, 141.
(3) Yin, Y. D.; Alivisatos, A. P. *Nature* **2005**, *437*, 664.
(4) Libbrecht, K. G. *Rep. Prog. Phys.* **2005**, *68*, 855.
(5) Seidel, H.; Csepregi, L.; Heuberger, A.; Baumgärtel, H. *J. Electrochem. Soc.* **1990**, *137*, 3612.
(6) Novoselov, K. S.; Geim, A. K.; Morozov, S. V.; Jiang, D.; Zhang, Y.; Dubonos, S. V.; Grigorieva, I. V.; Firsov, A. A. *Science* **2004**, *306*, 666.
(7) Geim, A. K. *Science* **2009**, *324*, 1530.
(8) Li, X.; Cai, W.; An, J.; Kim, S.; Nah, J.; Yang, D.; Piner, R.; Velamakanni, A.; Jung, I.; Tutuc, E.; Banerjee, S. K.; Colombo, L. G.; Ruoff, R. S. *Science* **2009**, *324*, 1312.
(9) Yu, Q. K.; Jauregui, L. A.; Wu, W.; Colby, R.; Tian, J. F.; Su, Z. H.; Cao, H. L.; Liu, Z. H.; Pandey, D.; Wei, D. G.; Chung, T. F.; Peng, P.; Guisinger, N. P.; Stach, E. A.; Bao, J. M.; Pei, S. S.; Chen, Y. P. *Nat. Mater.* **2011**, *10*, 443.
(10) Wu, B.; Geng, D. C.; Guo, Y. L.; Huang, L. P.; Xue, Y. Z.; Zheng, J.; Chen, J. Y.; Yu, G.; Liu, Y. Q.; Jiang, L.; Hu, W. P. *Adv. Mater.* **2011**, *23*, 3522.
(11) Geng, D. C.; Wu, B.; Guo, Y. L.; Huang, L. P.; Xue, Y. Z.; Chen, J. Y.; Yu, G.; Jiang, L.; Hu, W. P.; Liu, Y. Q. *Proc. Natl. Acad. Sci. U.S.A.* **2012**, *109*, 7992.
(12) Xie, L. M.; Jiao, L. Y.; Dai, H. J. *J. Am. Chem. Soc.* **2010**, *132*, 14751.
(13) Yang, R.; Zhang, L. C.; Wang, Y.; Shi, Z. W.; Shi, D. X.; Gao, H. J.; Wang, E. G.; Zhang, G. Y. *Adv. Mater.* **2010**, *22*, 4014.
(14) Shi, Z. W.; Yang, R.; Zhang, L. C.; Wang, Y.; Liu, D. H.; Shi, D. X.; Wang, E. G.; Zhang, G. Y. *Adv. Mater.* **2011**, *23*, 3061.
(15) Xie, G. B.; Shi, Z. W.; Yang, R.; Liu, D. H.; Yang, W.; Cheng, M.; Wang, D. M.; Shi, D. X.; Zhang, G. Y. *Nano Lett.* **2012**, *12*, 4642.
(16) Vlassiouk, I.; Regmi, M.; Fulvio, P.; Dai, S.; Datskos, P.; Eres, G.; Smirnov, S. *ACS Nano* **2011**, *5*, 6069.
(17) Zhang, Y.; Li, Z.; Kim, P.; Zhang, L.; Zhou, C. *ACS Nano* **2012**, *6*, 126.
(18) Campos, L.; Manfrinato, V.; Sanchez-Yamagishi, J.; Kong, J.; Jarillo-Herrero, P. *Nano Lett.* **2009**, *9*, 2600.
(19) Datta, S. S.; Strachan, D. R.; Khamis, S. M.; Johnson, A. T. C. *Nano Lett.* **2008**, *8*, 1912.
(20) Ci, L. J.; Xu, Z. P.; Wang, L. L.; Gao, W.; Ding, F.; Kelly, K. F.; Yakobson, B. I.; Ajayan, P. M. *Nano Res.* **2008**, *1*, 116.
(21) Schumacher, C. M.; Koehler, F. M.; Rotzetter, A. C. C.; Raso, R. A.; Stark, W. J. *J. Phys. Chem. C* **2012**, *116*, 13693.
(22) Wu, B.; Geng, D. C.; Xu, Z. P.; Guo, Y. L.; Huang, L. P.; Xue, Y. Z.; Chen, J. Y.; Yu, G.; Liu, Y. Q. *NPG Asia Mater.* **2013**, *5*, No. e36.
(23) Wang, H.; Wang, G. Z.; Bao, P. F.; Yang, S. L.; Zhu, W.; Xie, X.; Zhang, W. J. *J. Am. Chem. Soc.* **2012**, *134*, 3627.
(24) Gao, L. B.; Ren, W. C.; Xu, H. L.; Jin, L.; Wang, Z. X.; Ma, T.; Ma, L. P.; Zhang, Z. Y.; Fu, Q.; Peng, L. M.; Bao, X. H.; Cheng, H. M. *Nat. Commun.* **2012**, *3*, 699.
(25) Vicsek, T. *Fractal Growth Phenomena*; World Scientific: Singapore, 1992.
(26) Zhang, Z. Y.; Lagally, M. G. *Science* **1997**, *276*, 377.